Influence of cathode grid geometry upon mode structure of a Transparent Cathode Discharge

T. Hardiment[1, a)] and M. D. Bowden[1, b)]
Department of Electrical Engineering and Electronics, University of Liverpool, Liverpool L69 3GJ, UK

(Dated: 14 February 2020)

We measured current-voltage and optical emission for self-sustained discharges obtained using two forms of cylindrical wire grid cathode, having either an enclosed or an open end. Enclosure of the open end extended the low-pressure range for a 'cathode-confined' or CC mode, from around 12.5 Pa to below 3.5 Pa, conditions at which a 'beam' mode discharge otherwise occurs. The modification also caused dark space to envelop the glow within the cathode, bridged by bright emission resembling plume for the CC mode, and electron beam for the beam mode. We explain these results by treating the CC mode as a hollow cathode discharge, for which only γ-electrons that suffer inelastic loss before escaping the cathode grid are significant. For the two cathodes, respective degrees of electron confinement possible for the different sheath configurations predict the low-pressure ranges, and calculated values of cathode fall for self-sustenance by the hollow cathode effect agree approximately with experimental voltages across a range of pressures. Plume- and beam-like forms of emission indicate inherently different electron energies, consistent with bulk transport across potential distributions characteristic to mode. Where these features bridge the enclosed cathode boundary, this shows existence of an otherwise closed potential surface within the cathode, confirmed by geometry of the plume-CC mode configuration, where relation between main glow and plume interface surfaces indicates the arrangement to self-organise in a state of non-ambipolar current flow. Similarities in mode structure reported elsewhere for related discharges indicates the findings to be relevant for these also.

I. INTRODUCTION

The aim of this paper is to establish further understanding of modes of glow discharge operation that may occur at low pressures in apparatus with a hollow grid cathode. This type of device, often referred to colloquially as a fusor, was first researched in the 1950s and 60s as part of the Inertial Electrostatic Confinement (IEC) approach to fusion energy. Early IEC work used a spherical grid electrode, variously as anode or cathode, to inject charged particles into a central region at conditions of very low pressure[1–3]. Theory based upon collisionless particle flow predicted complex space charge structures to form[4–6], that would confine and heat fuel ions to provide high reaction rates. Such high-gain operation has not yet been realised, despite continuing innovation and research[7–9], and fusion efficiencies for laboratory IEC devices remain 10^{-7} or smaller. Since the 1990s much IEC research has investigated relatively simple devices operating in the glow discharge regime. Most of this work has been directed toward non-power fusion application as sources of MeV protons and neutrons, e.g.[10,11]. Other research has considered non-fusion application as spacecraft thrusters, that might utilise either the fast neutral products of charge exchange reactions[12] or jets and beams that occur at certain operating conditions[13–17]. For this work a spherical or cylindrical grid cathode is generally operated at sufficiently high pressures for a self-sustained discharge to occur, that has been called a transparent cathode discharge (TCD)[18,19]. We use this term since it conveniently describes both the electrode configuration and operating regime.

a)tom.hardiment@gmail.com
b)mark.bowden@liverpool.ac.uk

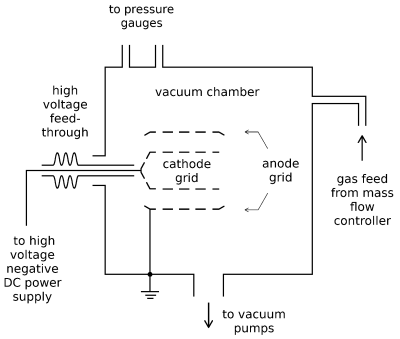

FIG. 1. Layout of vacuum chamber used for our experiments. The two co-axial grid electrodes are shown approximately to scale with the cube-shaped chamber.

TCDs are known to operate in a variety of different modes, that have been characterised in the literature according to patterns of optical emission, as 'spray' or 'spray jet', 'jet' or 'tight jet', 'halo', 'central spot' and 'star' modes[15,18,20,21]. Current-voltage behaviour, plasma properties, dependences upon electrode geometry and fusion reactivity are recorded for some of these, although the IEC and TCD literature contains no definitive account of fundamental processes that underpin the reported mode structure. Different sustaining and self-organisation mechanisms entail characteristic potential distributions and discharge properties, and since these will determine utility for different applications, practical interests

lie in the identification of physical processes underlying different modes, and in understanding the influence of device configuration upon conditions at which these may operate. Fusion yields for lower-pressure modes such as 'star' and 'halo' modes indicate these to be associated with the activity of energetic ions and neutrals[20,21], and higher-pressure discharges within an IEC cathode have been described variously as hollow cathode type-discharges[4] and spherical double layer (SDL) structures[16,17]. These types of plasma have been extensively researched in other fields[22–28], and devices with transparent electrodes have also been studied outside of the IEC context. In some of these cases, positively-biased wire grids have been operated within an externally generated plasma[29,30]. In others a mesh cathode has been used to generate self-sustained discharges[31–37], for which apparatus and conditions are more analogous to TCDs, and we shall consider our experimental results in this wider context.

In a previous study of a TCD obtained in a set-up with an open-ended cylindrical grid cathode surrounded by a grounded anode grid[19] (Figs. 1, 2) we examined optical emission from two principal modes evident at pressures of helium smaller than 100 Pa, and found these to represent discharges sustained by the activity of energetic electrons at conditions of higher pressure/lower voltage, and ions and neutrals at lower pressure/higher voltage. Observed in various gas species, this broad mode structure is the manifestation of a universal progression of different regimes of reduced electric field, *E/n*, at which electrons and the much-heavier ions and neutrals (that we shall refer to as 'heavy particles') gain reactive energies. We called the low-pressure discharge the 'beam' mode, since visible emission in this mode takes the appearance of radial beams of heavy particle-induced emission that pass diametrically through apertures of both grids, and an axial electron beam that occurs between the cathode and chamber wall. The electron-driven mode, that we called the 'cathode-confined', or 'CC' mode, showed characteristics of a discharge sustained by the hollow cathode effect, that occurs as energetic electrons emitted from the cathode under ion bombardment become confined within the field structure between plasma and cathode[22,23]. We projected the low-pressure limit for this mode in our apparatus to be determined by loss of such electrons via the open end of the cylindrical cathode, affording insufficient electron confinement to extend electron-driven operating conditions from conventional *E/n* suggested in the literature. This apparent dependence upon cathode form however suggests the influence of the hollow cathode effect will vary for different cathode geometries, and so electrode construction may determine conditions at which TCD properties will be analogous to those of hollow cathode discharges.

In this paper, we investigate the influence of cathode form upon this mode structure, by observing the effect of enclosing the open cathode end with further wire grid-work. The description concentrates principally upon the discharge in helium, since the mode structure is well-defined in terms of both electrical characteristics and optical emission. After description of the experimental apparatus in Section II, we describe measurements of optical emission distributions and electrical characteristics in Section III. The results are analysed and discussed in Sections IV and V.

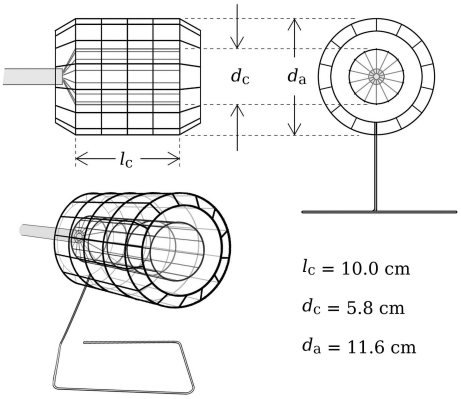

FIG. 2. Form and dimensions of the standard electrode assembly, with open-ended cathode positioned inside the grounded anode.

II. EXPERIMENTAL APPARATUS

Our experimental apparatus has been described previously[19], and in the following summary we also describe the modification made to the cathode for this work. The experiment is contained within a cube-shaped vacuum chamber with 30 cm sides, five of these are stainless steel and the top is acrylic with glass shielding. A viewport window is fitted to one of two larger ports, services and diagnostics to others. The system is evacuated using a Leybold Turbovac50 turbo-molecular pump, backed by an Edwards RV3 rotary vane pump, with base pressure of around 10^{-3} Pa. Gas may be admitted into the chamber via MKS mass flow controllers, and pressure is monitored using either a Pfeiffer capacitance manometer for pressures lower than around 12 Pa, or a Pfeiffer dual pirani gauge for higher pressures.

In our standard experimental set-up, the chamber contains two cylindrical, coaxially-arranged grid electrodes, with the cathode positioned inside the anode. Both electrodes have fourteen apertures around the circumference, and are made from 1.6 mm diameter stainless steel. The cathode is 10 cm in length, with radius a little less than 3 cm, half that of the anode. One end of the cathode is open, and the other enclosed by wire struts. These are attached to the high-voltage feedthrough, that also serves as cathode support. The anode is supported by a simple stainless steel stand, and has an additional row of apertures at each end giving it a barrel-shaped appearance. The anode grid is held close to ground by a small resistance, so that this electrode and the grounded chamber both act as anode for the discharge. Fig. 2 shows a sketch of this electrode arrangement. For the experiment described in this paper, we wished to observe the effect of enclosing the

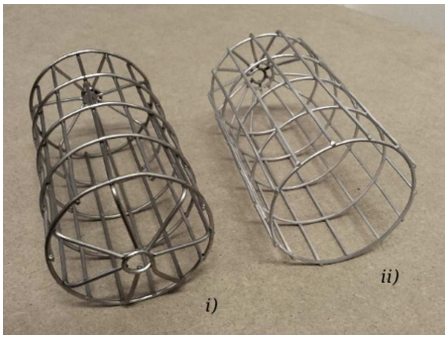

FIG. 3. Photograph showing i) the enclosed, and ii) the open-ended grid cathodes used for experiments described in this paper. Both electrodes are made from 1.6 mm diameter stainless steel wire (surfaces appear different since only ii) had been sputtered in operation).

open cathode end. This was done by constructing an alternative cathode, for which both ends were enclosed by wire struts (Fig. 3). This second electrode was constructed using half the number of wire struts for each end, so that the degree of enclosure was altered without changing the geometric transparency. In the following we shall refer to the original cathode as the 'open-ended' cathode, and the other as the 'enclosed' cathode. Either cathode could be fitted to the experimental apparatus described previously, without further change to the set-up.

The cathode was driven by a Glassman WX series negative DC power supply, capable of sinking 100 mA at voltages up to 10 kV. Limiting values for current and voltage may be independently configured, and the unit operates in either a voltage- or current-controlled mode, according to which set parameter limits the output. For the work described in this paper, the current limit was set to maximum and voltage varied manually, so that the dependence of current upon voltage was observed. The power supply outputs analogue monitoring signals, that were sampled using the analogue-digital conversion (ADC) functionality of an Arduino microcontroller board in order to record measurements of voltage and current. The ADC has a 10-bit resolution, corresponding to around 0.1 % of full scale. Current-voltage relations were recorded using the following procedure: after operation for a short conditioning time, voltage was ramped up and down over a period of a few seconds, with values of current and voltage sampled and recorded at tens of Hz. This technique records many values, including fluctuations corresponding to power supply regulation, and the results shown in Section III have some points removed for clarity. Optical emission distributions were recorded using standard imaging cameras.

III. EXPERIMENTAL OBSERVATIONS

This section contains measurements and observations of discharges operated in helium and argon, using the two different cathodes. Part III A contains measurements of electrical properties while Part III B contains images that show both the generic appearance of the discharges and some distinctive features observed for specific operating conditions. In both sections, we concentrate on the appearance and the behaviour of the cathode-confined mode of the discharge.

A. Current-voltage behaviour

Figure 4 shows current-voltage measurements for the two systems, recorded in each case for a range of pressures. The results shown for the open-ended cathode in Fig. 4 i) are similar to those we have reported previously[19], and the same interpretation can be applied. The results in the upper left of the figure correspond to beam mode discharges, the results in the lower right of the figure correspond to cathode-confined discharges and the arrows on the figure indicate discontinuities in the I-V curves that are associated with transitions between the two modes. The discontinuities are observed during the increasing part of the curve, and we previously observed these to be consistent with the increased ionisation efficiency associated with operation of the hollow cathode effect. During ramp-down a significant hysteresis occurs. For curves shown in Fig. 4 this causes the discharge to persist in the cathode-confined mode until the discharge extinguishes, although we have observed transition back to the beam mode for lower pressures in the range[19].

Fig. 4 ii) shows I-V curves measured from discharges with the fully enclosed cathode. In some respects, the results are qualitatively similar to those for the case of the open-ended cathode such as the beam mode occurring at lower-pressure and/or lower-current conditions, cathode confined mode for higher-pressure and/or higher current cases, and discontinuities and hysteresis associated with the transition between the modes. However, there are important differences.

For the open-ended cathode, I-V discontinuities were observed for pressures between around 33 Pa and 13 Pa, and for the enclosed cathode between 13 Pa and 5 Pa. Not only is the low-pressure range for the cathode-confined mode different for each cathode, but the discharge behaves differently in the low-pressure limit. With the open-ended cathode, the mode ceases to appear at pressures below around 12.5 Pa. With the enclosed cathode, the mode may persist at pressures above 5 Pa, but also appears to instigate at pressures significantly lower than this. This was observed at pressures as low as 3.5 Pa, which was the lowest pressure tested. In this extra-low-pressure range, the mode extinguishes almost immediately and then re-instigates, causing a flickering effect. The low-pressure limit for this behaviour was not ascertained.

The results shown in Fig. 4 are from helium discharges. In our previous study[19] we found a qualitatively similar mode structure to occur in both helium and argon for the open-ended cathode, and so the effect of cathode enclosure was observed for argon also. When the apparatus with enclosed cathode was operated in argon, the cathode-confined mode was observed to form at pressures as low as 0.5 Pa, compared with a low-pressure limit of around 2.5 Pa for the open-ended cathode.

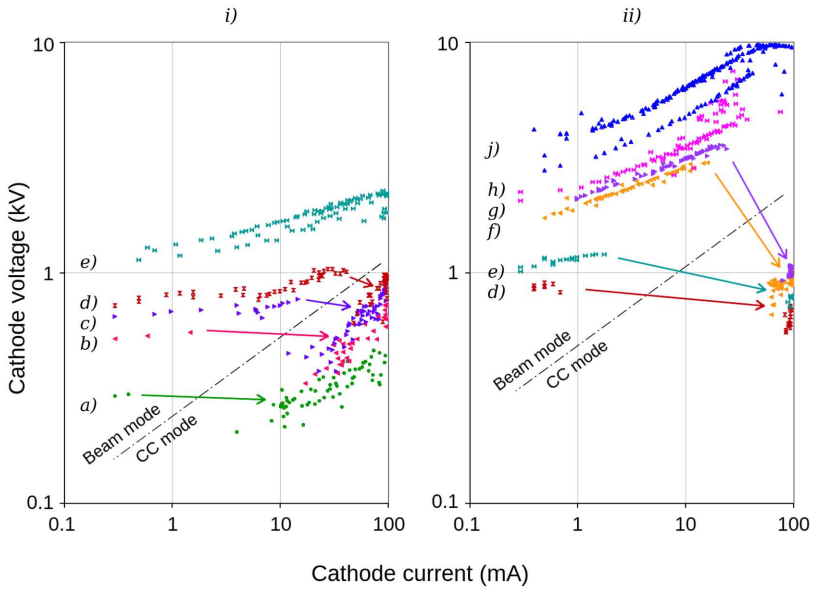

FIG. 4. Current-voltage curves in helium for apparatus with i) open-ended cathode and ii) closed cathode, corresponding to pressures: a) 32 Pa; b) 18 Pa; c) 15 Pa; d) 14 Pa; e) 10 Pa; f) 5.9 Pa; g) 5.5 Pa; h) 4.9 Pa; j) 3.5 Pa. Arrows represent discontinuities occurring upon appearance of the CC mode, as voltage was increased. The mode exhibits a strong hysteresis, and generally persists until extinction of the discharge as voltage is reduced (colour online).

In this respect, the discharge showed broadly similar characteristics to the helium results, with the low-pressure limit for the cathode-confined mode considerably smaller for the enclosed cathode. With the enclosed cathode, we also observed the transition to the CC mode to generally occur at comparatively low threshold currents, making it hard to operate the beam mode discharge in argon at significant power using this electrode.

B. Distributions of optical emission

The electrical measurements in III A show that, for both electrode cases, the discharges can be identified as operating in either the cathode-confined mode or the discharge mode we have called the beam mode. While this mode structure is distinct for either set-up, there are significant differences in discharge behaviour within the regimes, and to describe these it is helpful to examine the physical appearance of the discharge as well as its electrical nature. Figure 5 shows the characteristic appearance of discharge modes that occur for each electrode arrangement, when operated at two significantly different pressures. For each electrode, images show cathode-confined and beam mode discharges at respective conditions of high and low pressure, and also examples of each mode occurring at same pressure. We show images of the discharge with open-ended cathode on the left-hand side of Fig. 5 [i), iii) and v], and images with enclosed cathode on the right [ii), iv) and vi)]. Upper left images [i)–iii)] represent discharges at 18-20 Pa, and lower right [iv)-vi)] show discharges at ∼7 Pa. Minor adjustments have been made to brightness and contrast for individual images, so that discharge appearance is consistently represented within the figure.

Fig. 5 i) and ii) show the cathode-confined mode discharges for both electrode cases, observed for similar pressures of 18-20 Pa. In both cases, emission is observed within a central region of the cathode interior, surrounded by a dark space between the glow and the cathode itself. For the open-ended cathode the glow diverges as it extends into the chamber outside the electrode, becoming dimmer and more diffuse. For the enclosed cathode the central glow is entirely surrounded by dark space, except at the end of the cylindrical electrode, where a plume-shaped glow extends into the open chamber. The plume appears to be attached to the inner glow, and passes through one of the apertures in the cathode. This discharge configuration (Fig. 5 ii)) is observed to appear over a wide range of conditions of both cathode current and pressure, and is characteristic of the cathode-confined mode for the enclosed

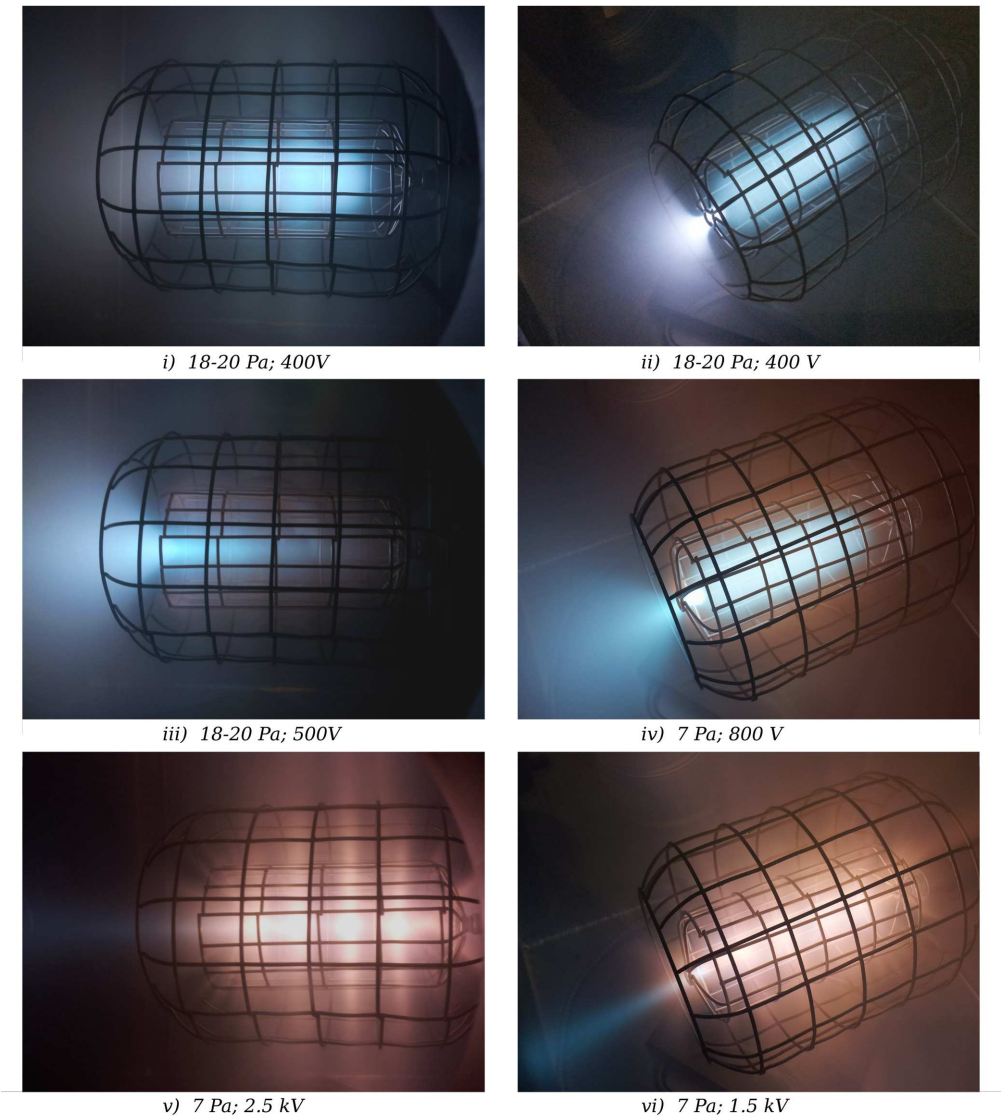

FIG. 5. Discharges in helium obtained using i), iii) and v) the open-ended cathode, and ii), iv) and vi) the enclosed cathode. For either electrode case, these photographs show the mode states evident for two sets of conditions, representing higher and lower pressure. Characteristic distributions of emission are shown for discharges operating in the CC mode at high pressure in i) and ii), and in the beam mode at low pressure in v) and vi). Discharges shown in iii) and iv) represent beam mode operation at high pressure, and CC mode operation at low pressure, for apparatus where these states may occur (colour online).

cathode. At lower levels of cathode current, two or three plumes have been observed, that often appear to flicker.

Fig. 5 v) and vi) show the beam mode at ∼7 Pa for both electrodes. As was discussed in our previous work, the beam mode with open-ended cathode is characterized by a series of radial beams that extend from the interior of the cathode through the apertures in the cathode and out towards the chamber walls. As well as these radial beams, Fig. 5 v) shows an axial beam that extends from the open end of the cathode. For the beam mode in the enclosed cathode, shown in Fig. 5 vi), it can be seen that the axial beam appears significantly brighter than that observed with the open-ended cathode. As for the plume accompanying the CC mode discharge with this electrode, the beam originates within the cathode and passes through an aperture, to then continue in a straight line to the wall, where significant local heating causes the 10 mm stainless steel to become very hot in minutes.

To understand the formation of the cathode-confined mode in each electrode arrangement, it is useful to examine the conditions just before and just after its formation, to see the transition from beam mode to cathode-confined mode. Fig. 5 i) and iii) show the discharge in the open-ended cathode to either side of the mode transition, at 18-20 Pa. Towards the upper pressure limit the 'beam' mode discharge does not take the characteristic appearance described for lower pressures, instead consisting principally of a large axial plume-shaped glow that extends from the open cathode end. Fig. 5 iv) and vi) are images showing the transition from beam mode to cathode-confined mode for the enclosed cathode, at 7 Pa. Fig. 5 iv) shows the discharge after transition to the cathode-confined mode. It can be seen that the axial beam is replaced by the plume-shaped formation characteristic of cathode-confined mode at higher pressure [as in Fig. 5 ii)]. There is no image of enclosed-cathode beam mode at 18-20 Pa, or open-ended CC mode at 7 Pa, since such states do not occur at these pressures.

Much emission from the helium discharges illustrated in Fig. 5 appears green or orange to the eye, the green colour reproducing in these photographs as green/blue. In our previous work[19], we found this distinctive emission structure to result as either electrons or heavy particles gain reactive energies at different *E/n* conditions. The green colour is caused as electron-impact excitation to 3^1P results in significant emission at 501.6 nm, and the orange emission occurs primarily at 587.6 nm after heavy particle collisions cause excitation to 3^3D. This arises due to very different magnitudes of respective cross sections, and is made visually unambiguous for energetic species at conditions of relative low pressure by the difference in wavelength, and generally sparse helium spectrum. For conditions illustrated in Fig. 5, distributions of these colours may therefore be associated with the local presence of energetic electrons and heavy species. These will also generally coincide with regions of smaller and greater respective *E/n*, although since fast neutrals may propagate regardless of field structure, these may cause emission away from the region of ion acceleration. Orange emission is only significantly present for the lower pressure discharges Fig. 5 iv)-vi), occurring principally within the inter-electrode region and also within the cathode for beam mode states. For these discharges the axial beam or plume-type features remain green, as does the glow within the cathode for the low-pressure CC mode (Fig. 5 iv)). At higher-pressure conditions the CC mode glow appears green in both electrode cases, with the axial plume appearing paler.

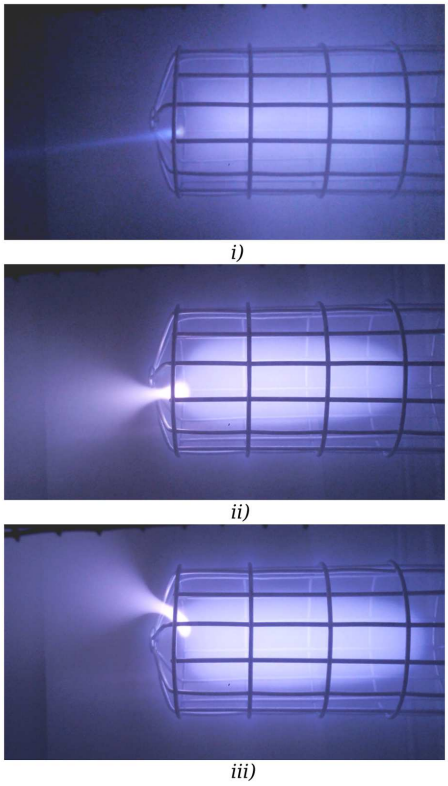

FIG. 6. Discharges in argon at 1 Pa, showing i) beam and ii)-iii) plume formations associated with the enclosed cathode. All three images were obtained from the same perspective, and ii) and iii) illustrate how the plume may appear from different apertures of the cathode (colour online).

In argon, spatial distributions of emission observed for the CC and beam modes were similar to those described above for helium. These general similarities were evident for operation with both the open-ended cathode and the enclosed cathode, the cathode modification causing principal effects for either species.

In the images shown for helium in Fig. 5, the perspective makes details of these features hard to see, and so the discharge was also operated (in argon) with the enclosed cathode and without the anode grid, enabling clearer observation

of beam and plume structures. A detailed investigation was not carried out for this arrangement, and we did not quantify the effect of using only the chamber wall as anode. The CC mode was however observed to occur at broadly similar conditions of pressure and voltage, and significantly for our purpose here the plume and beam features were evident in the same way. We show images obtained during this run in Fig. 6, these are generally representative of structures occurring in either species, and with or without the anode grid.

Dimensions of the plume and beam appear to be largely independent of current or pressure, although parts of each feature where these cross the cathode boundary appear consistently narrower in argon than in helium. For either species, a small region of relatively intense emission that contacts the cathode interior glow is considerably smaller for the beam than for the plume. The entire structure of the beam feature is co-linear and oriented normal to the plane of the aperture, expanding in width as it crosses the boundary. In contrast, the plume narrows within the aperture, before curving and expanding to contact the CC mode glow in a more globular interface. We observed some variation in shape of this at different conditions of current, although the overall size of the feature varied little.

C. Mode transition

At certain conditions during operation with the enclosed cathode, an evolution in the discharge was observed to occur whilst no adjustment was made to the apparatus, that resulted in a more gradual transition to the CC mode. In general the CC mode occurs spontaneously, either at breakdown or as levels of voltage and current are actively increased, but at pressures below around 7 Pa in helium, levels of cathode current were observed to gradually increase whilst voltage was kept constant. For the helium discharge, the colour of emission within the cathode interior was also observed to change during this process, becoming progressively more green, until transition to the CC mode occurred. A rise in current similar to this may be observed in the current-voltage curve obtained using the enclosed cathode at 3.5 Pa, in Fig. 4 ii).

IV. ANALYSIS

Enclosing the open cathode end caused the cathode-confined mode plasma to appear additionally surrounded by cathode sheath, and also to occur at significantly lower pressures. These properties are consistent with enhanced confinement of energetic electrons occurring within a more extensive sheath structure, and so agree with our previous analysis for the open-ended cathode[19]. In the following Section IV A we consider extension of this to describe the observed effects of cathode modification, and the hollow cathode effect more generally for grid cathode discharges. We shall then consider how emission distributions occurring in the different electrode arrangements relate to discharge configurations of potential and current, in IV B.

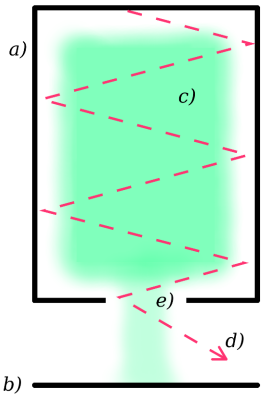

FIG. 7. Sketch of conventional hollow cathode discharge showing a) cathode cavity, b) anode, c) plasma, and d) confined trajectory for a γ-electron, emitted at top centre, and reflected several times within the plasma-cathode fall before exiting the cavity via aperture e) (colour online)

A. The hollow cathode effect in grid electrodes

We first outline some principal properties that enable hollow cathode discharges (HCDs) to operate at low pressures, referring throughout to a review of the 'electrostatic electron trapping' or 'hollow cathode' effect[23]. For a discharge to self-sustain, electrons emitted from the cathode under ion bombardment, that we refer to as 'γ-electrons' after the second Townsend coefficient γ, must subsequently cause sufficient ionisation for the resulting ion flux to replace them. This condition may be expressed in terms of M, the average multiplication factor required for all γ-electrons emitted:

$$M = 1/\gamma + 1 \tag{1}$$

The hollow cathode effect (HCE) occurs as γ-electrons emitted from the inner surface of a cathode cavity, held at voltage V_C, become reflected in opposing cathode falls of magnitude V_{CF} until they exit the cavity, causing relative increase of their trajectories within the discharge (Fig. 7). This confinement of energetic electrons results in an enhanced efficiency of ionisation, that may assist a discharge to occur at additionally low pressures. The configuration illustrated in Fig. 7 is known as the 'conventional' hollow cathode discharge, which resembles our discharges in having no physical anode within the cathode cavity. Optimal conditions exist for the HCE when γ-electrons lose all possible potential energy to ionisation before escaping the electrostatic trap. At these conditions V_{CF} must be sufficient for γ-electron multiplication to satisfy (1), and is independent of pressure. The fields important in the sustaining of the discharge occur in an otherwise field-free region,

and cathode voltage is characteristically of similar magnitude to V_{CF}. Expressions for M as a function of cathode fall, in the low pressure/long confined path regime, take the form:

$$M = \frac{eV_{CF}}{W}\left(1 + C\frac{d}{a}\frac{eV_{CF}}{W}\right) \quad (2)$$

in which d is sheath width, where e is fundamental charge and W represents electron energy cost per ionisation, around twice the ionisation potential for atomic gas species. a refers to distance travelled by a confined electron between reflections at the trap boundary, defined $a = 4V/S$, in which V refers to volume and S to surface area of the trap, so that d/a represents the proportion of a confined trajectory spent in the sheath. Different formulations of (2) have C as a constant between 0.13 and 0.5, or as a weak function of eV_{CF}/W returning 0.2-0.5 for eV_{CF}/W of 10-30. As a confined electron loses energy to inelastic collisions the ionisation length λ_{iz} varies considerably, but study of hollow cathode discharges has shown this may be well-approximated for electron energies within the range 50-500 eV as λ_0, an average path length between successive ionising collisions. This same value may conveniently be applied also for cathode fall larger than 500 V, since reduction in ionisation cross section is largely offset as greater ion energies impacting the cathode cause γ to increase above its γ_0 value. Towards the low pressure limit, the HCE becomes heavily reliant upon electron multiplication by ionisation in the cathode fall, and V_{CF} typically rises from hundreds to thousands of V. The extinction pressure for the discharge, P_{ex}, occurs where λ_0 exceeds the confined path length within the trap, L:

$$\lambda_0(P_{ex}) \sim L \quad (3)$$

The expression given for L is:

$$L = \frac{4V}{S_0} \quad (4)$$

in which S_0 refers to the part of the trap surface across which electrons may escape. This is valid for isotropic electron velocity distributions within cathode geometries of arbitrary form.

In our previous study[19] we considered the low-pressure limit for the helium CC mode in the open-ended cathode, making a simple adaptation to established HCD analysis to account for losses of γ-electrons through perforations of the grid. The approach taken was as follows. When (4) is evaluated for a largely transparent cathode, the grid-confined path L_G is similar to cathode diameter. This describes how in vacuum, most emitted γ-electrons will pass through opposing apertures to be lost. For conditions where a plasma exists within the cathode space however, electrons that suffer inelastic loss before reaching the boundary will be much more likely to become confined within the sheath structure. We suggested effective L for a grid electrode discharge might therefore be described by trapped path length within the plasma L_T, multiplied by probability for a γ-electron to become confined. Assuming average ionisation energy loss W to be sufficient for confinement by the sheath, probability for this was approximated as for a collision to occur before escaping the grid, expressed as the smaller of L_G/λ_{iz} or 1. We evaluated the LHS of (3) using $\lambda_0 = 1/n\sigma_0$ (where n is background gas density at 300K and σ_0 an average ionisation cross section size for 50-500 eV electrons in helium, of 3×10^{-17}cm^2), and calculated L_T from (4) by substitution of a value S_{0T} describing escape surface for confined electrons. This was approximated as the cross-sectional area of the open cathode end, making L_T around 44 cm. At the extinction pressure of 12.5 Pa, the cross section size derived from calculated λ_{iz} (around 23 cm) predicted an initial electron energy around 850 eV, consistent with V_{CF} similar to V_C. Probability for confinement L_G/λ_{iz} was around 0.25. At these conditions, λ_0 and effective L for emitted γ-electrons are of similar order to the distance between electrodes and chamber wall, and so the HCE may not extend the electron-driven discharge regime to significantly lower pressures in the set-up with open-ended cathode.

To consider our present results we shall apply the same principle, for an ionising collision to be necessary and sufficient for γ-electron confinement. The probability for this, that we defined as the smaller of L_G/λ_{iz} or 1, serves as an effective grid confinement parameter that is a function of grid geometry, pressure and cathode fall, and in the following we shall refer to this as Γ_G. To consider extinction pressures for the CC mode in the different cathodes, (3) becomes:

$$\lambda_0(P_{ex}) \sim \Gamma_G(P_{ex}, V_{CF})L_T \quad (5)$$

Whilst we only know P_{ex} to be smaller than 3.5 Pa for the enclosed cathode, we may calculate $P_{ex}(V_{CF})$ for both electrodes by finding values for which $\Gamma_G L_T/\lambda_0 \sim 1$. For this we use same σ_0 as previously, and the recommended function for $\sigma_{iz}(eV_{CF})$ from[38]. L_G is almost identical for either cathode. For S_{0T} in the enclosed cathode, we use the cross sectional area of the plume as this passes through the cathode aperture, judged to be a circular area around 0.8 cm diameter for the helium discharge. This makes L_T larger than for the open-ended cathode by a factor of around 50. Calculated values are shown in Fig. 8 for both cathodes, plotted against V_{CF} to which values of σ_{iz} correspond. The results broadly reproduce the different low-pressure ranges for the two cathodes, and so demonstrate how a more continuous sheath occurring within a more evenly-enclosed cathode may influence low-pressure range for the CC mode.

For a CC mode discharge sustained by the hollow cathode effect, little additional discharge potential should be required other than the cathode fall, and we may calculate V_{CF} in order to compare with experimental cathode voltage. We consider viability of a self-sustained cathode-internal plasma, assuming all ions to be generated within and collected by the cathode, and (1) to hold within the cathode interior. Since we consider initial confinement of γ-electrons to occur with probability Γ_G, a correspondingly larger multiplication factor M' will be required for those confined:

$$M \sim \Gamma_G M' \quad (6)$$

The RHS of (2) may be substituted for M' in (6), and combined with (1), giving:

$$\frac{1}{\gamma} + 1 = \Gamma_G\frac{eV_{CF}}{W}\left(1 + C_d\frac{eV_{CF}}{W}\right) \quad (7)$$

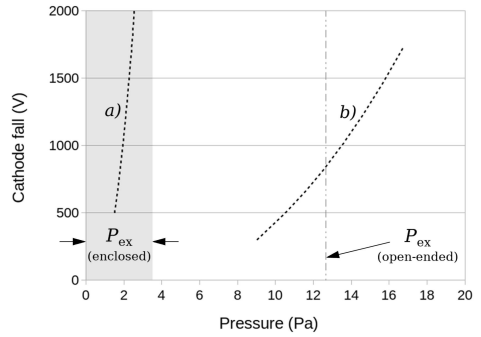

FIG. 8. Ranges of V_{CF}, P_{ex} satisfying (5) for a) enclosed cathode, and b) open cathode. Experimental P_{ex} for the open cathode is indicated, experimental P_{ex} for the enclosed cathode will lie within the shaded area

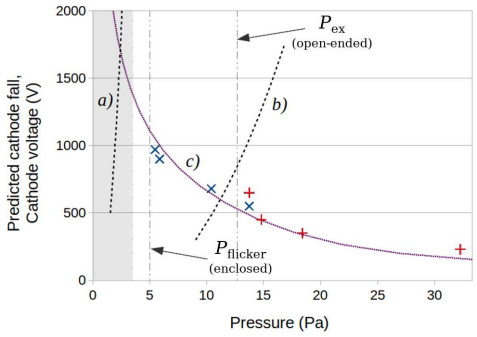

FIG. 9. Ranges of V_{CF}, P_{ex} satisfying (5) for a) enclosed cathode, and b) open cathode are reproduced from Fig. 8, with experimental cathode voltages, marked $\times$ for enclosed cathode; $+$ for open-ended cathode, shown against c) $V_{CF}(P)$ calculated using (7). Experimental P_{ex} for the open cathode and $P_{flicker}$ (threshold pressure for flickering in the enclosed cathode) are also indicated

We have incorporated the d/a term into C and given this a dependence upon eV_{CF}/W, redefining the term C_d for clarity and scaling values suggested for C in (2) by an appropriate value for d/a. This is estimated to be around 1/6, for d of 0.7-0.8 cm and with a calculated to be $\sim$4.65 cm for either electrode. A simple linear function $C_d = (eV_{CF}/W)/300$ returns values equivalent to $C = 0.2 - 0.6$ for eV_{CF}/W of 10-30.

We solved (7) for V_{CF} at a range of helium pressures, using values for $\sigma_{iz}(eV_{CF})$ as previously, and $\gamma = 0.2$[39], $W = 45$ eV for helium[22]. L_G varies by less than 1% for the two cathodes and so we do not distinguish between them. The results are compared in Fig. 9 with approximate lower cathode voltages at which the CC mode has been observed, taken from data in Fig. 4. Our observations were not made with the specific aim of measuring extinction voltage, and so the experimental values are not precise, but these generally agree well with results of the calculation, showing a broad trend for cathode voltage to increase at lower pressure that appears similar for either electrode. For the calculated values this pressure-dependence is introduced by Γ_G, since (7) otherwise describes optimal conditions, at which V_C and V_{CF} for HCDs are generally independent of pressure. An effect of cathode perforation is therefore introduction of a pressure-dependence for V_{CF} and V_C, that results as a γ-electron becomes less likely to play a role in the discharge at lower pressure. This effect operates in addition to the range-limiting effects of geometry of principal aperture and sheath configuration considered previously, and we expect these to cause the apparent increase in experimental voltage for the open-ended cathode in the low-pressure limit, as occurs for HCDs. The results shown in Fig. 9 also suggest explanation of the flickering observed for the enclosed cathode at pressures smaller than around 5 Pa, since calculated V_{CF} starts to become significantly larger here than for any other conditions, including the low-pressure operating range for the open-ended cathode. The flickering is therefore consistent with sufficient V_{CF} required at these conditions for cathode current to exceed the 100 mA supply limit.

The CC mode discharge is well-described by established principles of HCD operation, if we consider only γ-electrons that suffer inelastic loss before reaching the cathode boundary. This confirms the CC mode to be sustained by the HCE, and the low-pressure discharge mode structure to be determined by conditions at which such a plasma may exist within the cathode interior. The success of the approach indicates potential within cathode apertures, other than the open end, generally remains within W/e of cathode potential for the CC mode in our apparatus. Where this holds, approximate conditions of voltage and pressure at which a discharge mode may be sustained by the HCE are predicted for arbitrary cathode grid construction, which may assist identification of a hollow cathode-type mode within a grid cathode. In addition to establishing physical dependences for such a mode, identification of the sustaining mechanism also predicts discharge properties for such a mode will be analogous to those of conventional hollow cathode discharges. This provides insight for understanding potential distribution within the CC mode discharge, as consisting of a characteristic positive space charge within the cathode cavity with a potential relatively close to ground.

B. Emission distributions and discharge configurations

In the previous section we found the CC mode to be well-described as a discharge sustained by the hollow cathode effect, this explaining observed dependences upon conditions and electrodes, and predicting general similarities between properties of this mode and those of conventional HCDs. In the following we shall examine how this understanding may be applied to interpret the appearance of the discharge. We first consider how general distributions of emission may correspond to discharge configurations predicted for the two modes, before concentrating upon differences in emission

caused by the cathode modification.

In Section III B we noted visible colour of emission from helium discharges may provide a useful diagnosis of energetic species, with green emission at 501.6 nm principally occurring after excitation of the background gas by electrons, and orange emission at 587.6 nm after excitation by energetic ions and neutrals. Applying this understanding to discharges illustrated in Fig. 5, we observe significant activity of energetic heavy particles only at the lower-pressure conditions, and then in radial locations chiefly associated with the strong field between the electrodes. The CC mode glow is generally green and so associated with electron collisions, as is emission occurring in the axial region between electrodes and chamber wall, regardless of discharge mode or cathode format. This axial emission appears as either a beam or diverging plume, and in all instances appears to connect cathode internal discharge with the external chamber volume. In a discharge sustained by the hollow cathode effect, ionisation generates electrons in a region significantly enclosed by cathode fall much larger than electron temperature ($eV_{CF} \gg T_e$), and these must escape or accumulate to reduce eV_{CF} (see e.g.[40]). Our description of the CC mode as such therefore associates axial emission with transport of bulk thermal electrons from within the cathode interior, and the universal electron-impact emission signature for axial features, irrespective of mode, indicates these to perform this role generally.

For the emission distributions illustrated in Fig. 5, we observe a characteristic association between a plume-type axial structure and all instances of the CC mode. We also expect the potential difference across which bulk electrons are transported from CC plasma to chamber wall to be characteristically small, and so the association suggests plume- or beam-like appearance might result directly from the effect of respective potential distributions upon electron energies. Such interpretation of beam and plume form is consistent with properties of electron scattering in helium, where angle of scattering becomes significantly reduced at progressively greater electron energies (Fig. 10), and total elastic cross section becomes smaller by almost an order of magnitude as electron energy increases from 20 eV to 100 eV[41]. To place this in the context of our experiments, we calculate scattering mean free paths in similar manner as in the previous section; over the decade of helium pressures 3.2-32 Pa, these are approximately 5-0.5 cm for 20 eV electrons, and 45-4.5 cm at 100 eV. This means for a wide range of pressures relevant to our observations, lower-energy electrons will on average become deflected in collisions over the scale of the axial features, and electrons with greater energies will not. Distributions of trajectories leading to beam- or plume-like emission might therefore result from a simple variation in electron energy of this order, separately to any space charge repulsion or other field effects. If we associate the plume with a small gradient from the wall, the axial electron beam indicates a much larger potential difference between ground and the discharge within either cathode when operating in the beam mode. For the 'beam' mode discharge occurring at higher pressure in the open-ended cathode [illustrated in Fig. 5 iii)], the plume-type axial emission suggests a plasma potential that is also relatively close to ground,

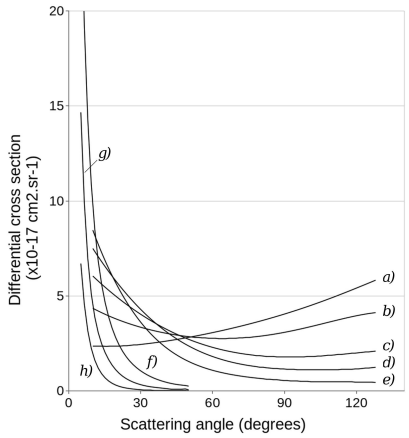

FIG. 10. Differential cross sections for elastic scattering of electrons in helium, at energies: a) 5 eV; b) 10 eV; c) 20 eV; d) 30 eV; e) 50 eV; f) 100 eV; g) 300 eV; h) 1 keV. Data taken from[42,43]

and that extends insufficiently far into the cathode for the CC mode to self-sustain.

To consider the effect upon distributions of emission caused by modification of the cathode end, we note this resulted in significant local changes for either mode, affecting the degree to which cathode-internal glow is enclosed by dark space, and causing bright emission associated with the axial features to cross the boundary of the enclosed electrode. The dark space between the CC mode glow and the cathode is the cathode sheath, which may become continuous when sheath width exceeds half the spacing between grid wires[44]. This condition is satisfied for the enclosed cathode geometry, where the dark space is interrupted only where the plume crosses the cathode boundary. The electron beam that occurs with the beam mode discharge in the enclosed cathode also constitutes the only bright emission to connect cathode-internal glow with the exterior region, and this indicates both structures to transport electrons across a potential barrier within the cathode boundary.

For such discharge configurations, geometry and potential will be constrained to maintain equilibrium currents of electrons and ions in steady state operation, and we may observe the effect of this by considering plasma dimensions for a CC mode discharge. The dependence of sheath configuration upon electrode surface ratios was first described by Langmuir[45], where an ion sheath occurring for a larger anode disappears for critical S_a, to become an electron sheath for smaller-sized anodes. More recent investigation has shown a state of 'non-ambipolar flow' to exist for equilibrium ratios of anode and cathode surfaces S_a and S_c, where an equal and opposite unipolar current flows across each surface from a plasma[46]. In this work, analysis of particle fluxes to anode and into an ion sheath of S_c, for a quasineutral plasma in which

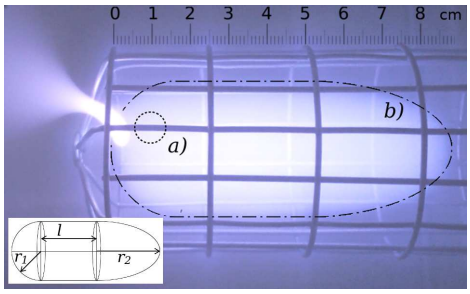

FIG. 11. Overlaid scale and (inset) geometry used to estimate CC mode plasma surfaces. Dotted line a) is a 2D circular area representing calculated interface area S_a; broken line b) outlines the boundary of 3D Bohm surface S_B. $\sim$ 1 Pa argon (colour online).

$T_e \sim 10T_i$, predicts the non-ambipolar state to exist for the ratio of surfaces, $\mu \leqslant S_a/S_c \leqslant 1.7\mu$, where critical surface ratio $\mu = \sqrt{2.3m_e/m_i}$ (m_i and m_e refer to ion and electron mass).

In Fig. 11 the CC mode argon discharge shown previously as Fig. 6 iii) is overlaid with a scale calibrated to cathode dimensions; this corresponds to the vertical plane on-axis and no correction is made for foreshortening. Ions will be accelerated away from the plasma and into the sheath as they attain Bohm velocity, and the surface at which this occurs is assumed to approximately coincide with the extent of bright glow within the cathode. We call this surface S_B, and the interface with the plume S_a. In Fig. 11 the dashed line marked b) describes the approximate boundary of S_B modelled as an assembly of hemisphere, cylinder and hemispheroid, as indicated in the inset. Dimensions as defined in the figure are estimated to be $r_1 = 1.8$ cm, $r_2 = 3.8$ cm and $l = 3.3$ cm, making $S_B \sim 94$ cm^2.The dotted line marked a) in Fig. 11 represents a 2D circular area of similar size to S_a. At $\sim$0.8 cm in diameter, this area is a little greater than 0.5 cm^2, and so related to S_B by $S_B \approx \mu S_a$. The geometry of the configuration therefore shows the plume to act as a virtual anode for the CC mode plasma, and the discharge to operate in the non-ambipolar regime. Interestingly, electrons incident upon S_a are implied to be transported from the main plasma with no reflection, since significant reflection would require the interface area to be correspondingly larger. For the open-ended cathode, the sheath structure between cathode end and axial glow is expected to rather consist of a small voltage drop of order T_e, that will moderate bulk electron transport from the plasma to maintain equilibrium. The non-ambipolar sheath configuration is described to be more efficient for charge extraction[46], in cutting loss of energetic electrons to surfaces other than S_a whilst allowing unimpeded flow for the lower-energy bulk population. The geometry shown in Fig. 11 indicates the plume to self-arrange in such an optimal sheath configuration with the main plasma, and this demonstrates that only electrons, and not ions, are transported from the main plasma by this route.

Similar characteristics are described for conventional hollow cathode discharges operating at conditions of small cavity aperture[47,48]. For these, properties of the 'anode' sheath that occurs at the aperture are also significantly determined by ratio of aperture area, with an equilibrium occurring when $S_a \sim S_c\sqrt{m_e/m_i}$. For smaller S_a/S_c two states are possible; either a double layer of larger surface may act as plasma anode in front of the aperture, drawing electrons across a potential step of a few 10s V, or a positive sheath of larger potential occurs and the discharge operates in a 'high voltage' mode. By analogy, this indicates the plume-plasma interface to also be a double layer structure.

Extension of the electron beam to within the enclosed cathode interior for the heavy particle discharge [Fig. 6 i)] indicates existence of a positive space charge structure within the cathode for this mode also, and the beam to play a similar functional role to the plume in extracting thermal electrons across an otherwise continuous cathode fall. The consistent size of interface surface observed for the beam, that is largely independent of pressure or current, suggests a qualitatively similar geometric determination as that for the plume. These observations indicate positive and negative products of ionisation will also exit the region of positive potential inside the cathode across separate surfaces. The generally smaller size of the beam interface is expected to result from different conditions within the cathode, possibly associated with the lack of a clearly-defined cathode sheath. This mode appears analogous to the 'high voltage' mode described elsewhere for conventional hollow cathode discharges, that is characterised as an ion space charge rather than a plasma[23], and that has also been widely associated with an electron beam e.g.[22,49].

C. Mode transition

The CC mode typically appears instantaneously, either at breakdown or as sufficient voltage is applied, and conditions for the mode to exist include requirement for $\Gamma_G L_T > lambda_0$, and sufficient V_{CF} for the HCE to self-sustain. We have considered general appearance of the beam and plume features to be determined by the effect of potential distributions in the different modes, and research into similar mode structure occurring for conventional HCDs and other transparent cathode configurations has found electron outflow to actually be causally important for establishing the potential configuration within the cathode. For conventional HCDs with small cathode aperture, the hollow cathode mode has been associated with stability of a double layer/anode plasma system existing within the aperture[23], with a critical local ionisation rate required to maintain the anode plasma and avoid entering the high-voltage mode. Stability of such an arrangement has been suggested to require a potential step across the double layer that is sufficiently small for electrons accelerated across this to have energies below the value at which iz reaches a maximum (100 eV)[48]. Recent modelling work has demonstrated a similar importance of electrons exiting a hollow cathode aperture for determining the discharge mode[50], finding potential within the cathode to rely significantly upon the ionising activity of these as they cross the cathode-anode space. Fast imaging of the transition from jet to

spray mode in a spherical transparent cathode[15,16] has shown a burst of emission occurring both within the cathode and in the beam preceding appearance of the spray mode, consistent with sufficient ion production occurring in the beam for an anode plasma to establish. In the description of the non-ambipolar discharge regime[46], plasma potential is noted to remain 'locked' to that of the electron extraction surface, in this context suggesting that should potential along the electron extraction channel become similar to anode, this will act to pull up the plasma potential within the cathode.

We also described a more gradual transition from the beam mode that may occur when using the enclosed cathode. In this process an autonomous rise in current was observed at conditions of constant voltage, with simultaneous increasingly-green colour of emission within the cathode in helium signifying a rising rate of inelastic electron collisions occurring within the cathode[19]. The association indicates an increase in V_{CF} , that continues until this becomes adequate for the HCE to self-sustain. Why this growth in potential may occur on a timescale relatively much longer than the more usual behaviour is unclear.

V. DISCUSSION

We have shown how a hollow cathode-type mode may sustain in a very transparent cathode, and how conditions at which this is possible will depend upon format of the cathode. This indicates such a discharge mode will also occur for a variety of other perforated cathodes, in accordance with well-documented operation of the hollow cathode effect in other modified geometries known variously as cage, multi-rod and segmented configurations[22,23]. For transparent cathode discharges, the discharge efficiency associated with the hollow cathode effect means a discharge mode so sustained will tend to dominate where conditions allow, and the nature of the sustaining mechanism implies potential distribution, current-voltage and emission characteristics similar to those of a conventional hollow cathode discharge. Such distinctive characteristics will cause a common mode structure to be observed for various cavity-form cathodes, and we have already described various similarities evident between our results and conventional hollow cathode discharges. We find further parallels in the literature, both with discharges obtained using mesh cathodes of much finer pitch than our grid, and also with wire grid cathode discharges in the more usual spherical IEC geometry. Mesh cathodes were used for hollow cathode electron beam source work[31–35], although later work also used a conventional solid-wall configuration[51,52]. These investigations describe a similar mode structure, with the transition from a high-impedance electron beam mode to a low-impedance 'normal hollow cathode' mode also associated with a hysteresis. Other properties analogous to our results include a description of a 'runaway' build-up of current that results in transition to the low-impedance mode[32], and difficulties in operating the electron beam mode stably in argon[34,35]. This research placed emphasis upon properties of the electron beam mode, describing an essential dependence upon dark space external to the cathode[33,52], and measuring beam electron energies that indicated typical plasma potential within the cathode to be a few hundreds of V more positive than negative cathode voltages of kV[35]. More recent work with spherical mesh cathodes[36,37] has observed a mode structure with similar impedance change and hysteresis, and measured plasma potential in a low-impedance mode with plume-like feature to be close to ground for cathode voltage of several hundreds of V. The authors considered this mode sustained by the hollow cathode effect, and also noted parallels with IEC transparent cathode discharges. The modelling described in[50] sought to investigate results of this experimental work. From the IEC discharge literature, a similar change in discharge perveance and accompanying hysteresis is described for the transition between 'jet' and 'spray' modes reported for spherical transparent cathode discharges[15], and defining emission features for these modes also significantly resemble the plume and beam structures that we observe[15,53,54].

These extensive similarities indicate potential distributions characteristic of the hollow cathode mode structure to occur quite generally in these related sets of apparatus. For modes occurring in spherical IEC cathodes, this understanding is inconsistent with description of the spray mode glow as a spherical double layer (SDL) arrangement[16,17], since a SDL is not a self-sustaining discharge and has a magnitude of potential step across the double layer similar to the ionisation energy for the parent gas (see e.g.[26]). For the jet mode however, we note the glow boundary may appear well-defined within spherical grid cathodes[15,16,53,54], suggesting a sheath structure that is not present for beam mode discharges we describe here. A SDL structure, or 'fireball', has also been described to occur for mesh cathode discharges[36,37] as part of a plume-like feature contacting the cathode-internal glow. This identification was made by measurement of a potential difference at the interface similar to the gas ionisation energy, and observation of non-linear dynamic behaviour, referring to an extensive body of work examining these objects in different apparatus e.g.[25–28]. We will consider evidence for SDL objects occurring in our open-ended cathode discharges in a separate paper.

Our results may be useful for evaluating applications for transparent cathode discharges, both in facilitating identification of a hollow cathode discharge mode, and informing the engineering of mode transition pressure range by electrode design, should a mode of operation be desirable at particular conditions. For example, appearance of the CC mode at conditions otherwise associated with the ion/neutral-driven discharge would interrupt stable operation of a reactive plasma source intended to create a particular chemistry using energetic heavy particles, since this will will switch a significant part of the plasma properties to those of an electron-driven discharge. This may be observed directly in the change evident for emission colour within the enclosed cathode, where the orange heavy particle signature apparent for the beam mode in Fig. 5 vi) becomes green due to principal activity of energetic electrons for the CC mode in Fig. 5 iv). For our electrode arrangement, the open cathode end limits confinement of energetic electrons within the cathode-internal field structure, and so contributes significantly to the stability of the ion-

driven beam mode discharge at more moderate conditions of higher pressure and lower voltage. Confined path for electrons also depends upon relative dimensions of the cathode internal space, and so adequate electron escape will remain a design consideration for any larger-scale implementation of an open-ended cathode format. Our findings indicate the beam and plume to play a functional role in the unipolar extraction of thermal electrons from a virtual cathode region within the cathode interior, which may inform utility of these features for thruster applications[15–17]. In particular, ions produced within a cathode-internal plasma operating in a state of non-ambipolar flow, as illustrated for our discharge by geometry of the plume-plasma configuration in Fig. 11, will flow only to the cathode and not be ejected in the plume. This property is in apparent contradiction to interpretation of such features as intense space-charge neutralised beams of electrons and energetic ions[13,14]. For the plume that accompanies transparent cathode discharges operating in the CC or spray mode, the similarities with conventional hollow cathode discharges imply these will be unlikely to offer significant advantages over currently-used hollow cathode technology, the significant loss of γ-electrons via apertures of a grid cathode rather resulting in a reduced efficiency where such an electrode is used. Various applications for the electron beam have been previously investigated by the work in Refs.[31–35,51,52].

VI. CONCLUSION

In this study we investigated the dependence upon cathode form for the low-pressure mode structure of a transparent cathode discharge, by observing the effect of enclosing an open end of a cylindrical grid cathode. This was found to result in significant extension of the low-pressure range for the discharge mode we call the 'cathode-confined' or CC mode, and also caused the appearance of additional discharge features in the form of a beam and a plume that traverse cathode boundary and dark space in beam and CC modes respectively. In our analysis we have explained these discharge properties by considering the hollow cathode effect to be the mechanism responsible for sustaining the CC mode, extending our previous work that suggested initial confinement of a γ-electron to be well-represented by probability for an inelastic collision before escaping the grid. Ranges of possible extinction pressures calculated for the two cathode geometries agree broadly with experiment, although we were not able to measure the precise value for the enclosed cathode. We calculated cathode fall required for self-sustenance of the HCE as a function of pressure and cathode transparency, with values agreeing approximately with experimental voltage for either cathode. The analysis is expected to hold for a wide range of cathode grid forms, where suitable assessment is made of electron escape surface.

The efficiency associated with the hollow cathode effect makes this liable to dominate wherever conditions enable it to self-sustain, and this causes the similar mode structure widely reported for other transparent cathode discharges in spherical geometry, mesh cathode discharges and conventional hollow cathode discharges. Discharge properties associated with the CC mode and its analogues, that are called the 'spray', 'low-impedance' or 'hollow cathode' mode elsewhere, include a plasma potential relatively close to ground since the sustaining mechanism operates in the field between plasma and cathode. The beam and CC modes are therefore associated with characteristic distributions of potential in which voltage dropped from chamber wall to internal cathode plasma varies considerably, from a significant proportion of cathode voltage for the beam mode, to a small fraction of this for the CC mode. This predicts different characteristic electron energies within axial discharge features, that may explain the apparent beam and plume forms in terms of different effects of scattering and space charge. The extension of these structures to within the enclosed cathode interior indicates these to extract thermal electrons across a potential barrier caused by the electrode geometry, and comparison of surfaces across which electrons and ions are extracted from the CC mode plasma finds these to be related by a factor of $\mu = \sqrt{2.3 m_e/m_i}$. This indicates a state of non-ambipolar current flow to exist for the cathode internal plasma, in which an optimal sheath configuration causes all electrons to be extracted only by the plume and all ions to flow only to the cathode. The interface between plasma and plume for such a configuration is indicated to be a double layer structure, by analogy to similar structures occurring in conventional hollow cathode discharges. Whilst a brighter glow of similar extent is evident within the cathode for the electron beam mode, the plasma boundary is not well-defined, suggesting different discharge conditions within the cathode cause the characteristically-smaller beam-plasma interface. In operation with the enclosed cathode, the extended low-pressure range for the CC mode means this appears at conditions otherwise associated with the ion/neutral-driven discharge. This property will be unfavourable for any applications specific to heavy-particle operation, since a transition to the CC mode will cause plasma properties to become those of an electron-driven discharge. The form of the cathode grid is therefore a critical design parameter for the engineering of discharge mode structure. The functional role we ascribe to beam and plume in the extraction of thermal electrons from within the cathode interior, and the broad analogies drawn with related discharges, implies transparent cathode discharges operating in the spray mode are unlikely to offer significant advantages over currently-used hollow cathode technology for thruster applications.

ACKNOWLEDGMENTS

This work was supported by the Engineering and Physical Sciences Research Council, grant reference EP/L505018/1.

[1] O. Lavrent'ev, L. Ovcharenko, B. Safronov, V. Sidorkin, and B. Nemashkalo, "Jenergiya i plotnost'ionov v jelektromagnitnoj lovushke," Ukrain Fiz **8**, 440–445 (1963).
[2] P. T. Farnsworth, "Electric discharge device for producing interactions between nuclei," (1966), uS Patent 3,258,402.
[3] W. C. Elmore, J. L. Tuck, and K. M. Watson, "On the inertial electrostatic confinement of a plasma," Physics of Fluids (1958-1988) **2**, 239–246 (1959).

[4]R. L. Hirsch, "Inertial electrostatic confinement of ionized fusion gases," Journal of Applied Physics **38**, 4522–4534 (1967).
[5]P. T. Farnsworth, "Method and apparatus for producing nuclear-fusion reactions," (1968), uS Patent 3,386,883.
[6]R. M. Meyer, S. K. Loyalka, and M. A. Prelas, "Potential well structures in spherical inertial electrostatic confinement devices," IEEE Transactions on Plasma Science **33**, 1377–1394 (2005).
[7]T. McGuire and R. Sedwick, "Improved confinement in inertial electrostatic confinement for fusion space power reactors," Journal of Propulsion and Power **21**, 697–706 (2005).
[8]J. Park, N. A. Krall, P. E. Sieck, D. T. Offermann, M. Skillicorn, A. Sanchez, K. Davis, E. Alderson, and G. Lapenta, "High-energy electron confinement in a magnetic cusp configuration," Physical Review X **5**, 021024 (2015).
[9]S. Y. Gus' Kov and Y. Kurilenkov, "Neutron yield and lawson criterion for plasma with inertial electrostatic confinement," in *Journal of Physics: Conference Series 2016* (IOP publishing, 2016) p. 012132.
[10]G. H. Miley and J. Sved, "The iec star-mode fusion neutron source for naa—status and next-step designs," Applied Radiation and Isotopes **53**, 779–783 (2000).
[11]J. W. Weidner, G. Kulcinski, J. Santarius, R. Ashley, G. Piefer, B. Cipiti, R. Radel, and S. K. Murali, "Production of 13 n via inertial electrostatic confinement fusion," Fusion science and technology **44**, 539–543 (2003).
[12]L. Blackhall and J. Khachan, "A simple electric thruster based on ion charge exchange," Journal of Physics D: Applied Physics **40**, 2491 (2007).
[13]G. H. Miley, B. P. Bromley, and Y. Gu, "A novel iec propulsion unit for satellite applications," in *AIP conference proceedings*, Vol. 361 (American Institute of Physics, 1996) pp. 1435–1440.
[14]G. H. Miley, H. Momota, L. Wu, M. P. Reilly, V. L. Teofilo, R. Burton, R. Dell, D. Dell, and W. A. Hargus, "Iec thrusters for space probe applications and propulsion," in *AIP Conference Proceedings*, Vol. 1103 (American Institute of Physics, 2009) pp. 164–174.
[15]C. Syring and G. Herdrich, "Jet extraction modes of inertial electrostatic confinement devices for electric propulsion applications," Vacuum **136**, 177–183 (2017).
[16]Y. A. Chan and G. Herdrich, "Inertial electrostatic confinement: Innovation for electric propulsion and plasma systems," in *Proceedings of The 35th International Electric Propulsion Conference, Georgia Institute of Technology, USA* (2017).
[17]Y. A. Chan and G. Herdrich, "Influence of cathode dimension on discharge characteristics of inertial electrostatic confinement thruster," in *Proceedings of The 36th International Electric Propulsion Conference, University of Vienna, Austria* (2019).
[18]R. M. Meyer, M. A. Prelas, and S. K. Loyalka, "Experimental observations of a spherical transparent cathode glow discharge," IEEE Transactions on Plasma Science **36**, 1881–1889 (2008).
[19]T. Hardiment and M. D. Bowden, "Mode structure of a transparent cathode discharge," IEEE Transactions on Plasma Science **47**, 3124–3133 (2019).
[20]G. H. Miley, J. Javedani, Y. Yamamoto, R. Nebel, J. Nadler, Y. Gu, A. Satsangi, and P. Heck, "Inertial electrostatic confinement neutron/proton source," in *Dense Z-Pinches: 3rd International Conference 1994* (AIP Publishing, 1994) pp. 675–689.
[21]G. H. Miley, Y. Gu, J. M. Demora, R. A. Stubbers, T. A. Hochberg, J. H. Nadler, and R. A. Anderl, "Discharge characteristics of the spherical inertial electrostatic confinement (iec) device," IEEE Transactions on Plasma Science **25**, 733–739 (1997).
[22]R. R. Arslanbekov, A. A. Kudryavtsev, and R. C. Tobin, "On the hollow-cathode effect: conventional and modified geometry," Plasma Sources Science and Technology **7**, 310 (1998).
[23]V. Kolobov and A. Metel, "Glow discharges with electrostatic confinement of fast electrons," Journal of Physics D: Applied Physics **48**, 233001 (2015).
[24]L. P. Block, "A double layer review," Astrophysics and Space Science **55**, 59–83 (1978).
[25]M. Sanduloviciu and E. Lozneanu, "On the generation mechanism and the instability properties of anode double layers," Plasma Physics and Controlled Fusion **28**, 585 (1986).
[26]B. Song, N. D'Angelo, and R. Merlino, "On anode spots, double layers and plasma contactors," Journal of Physics D: Applied Physics **24**, 1789 (1991).
[27]R. Schrittwieser, C. Avram, P. C. Balan, V. Pohoata, C. Stan, and M. Sanduloviciu, "New insights into the formation of nonlinear space charge structures in various plasmas," Physica Scripta **2000**, 122 (2000).
[28]C. Ionită, D. Dimitriu, and R. W. Schrittwieser, "Elementary processes at the origin of the generation and dynamics of multiple double layers in dp machine plasma. internatl," Journal of Mass Spectrometry **233**, 343–354 (2004).
[29]R. Stenzel, J. Gruenwald, B. Fonda, C. Ionita, and R. Schrittwieser, "Transit time instabilities in an inverted fireball. i. basic properties," Physics of Plasmas **18**, 012104 (2011).
[30]R. Stenzel, J. Gruenwald, B. Fonda, C. Ionita, and R. Schrittwieser, "Transit time instabilities in an inverted fireball. ii. mode jumping and nonlinearities," Physics of Plasmas **18**, 012105 (2011).
[31]H. L. L. Van Paassen, E. C. Muly, and R. J. Allen, "Electron beam phenomena associated with perforated wall hollow cathode discharges," in *Proc. Nat. Electron Conf. JL8* (1962) p. 596.
[32]M. A. Cocca and L. H. Stauffer, "Grid controlled plasma electron beam (no," in *CONF-57-6; AED-Conf-63-031-12* (General Electric Co., Schenectady, NY (United States), 1963).
[33]L. H. Stauffer, "Modulated plasma electron beams," in *CONF-60-3; AED-Conf-63-128-1* (Advanced Technology Labs, General Electric Co., Schenectady, NY (United States), 1963).
[34]G. Ward, "A perforated hollow cathode electron beam gun," Vacuum **18**, 507–509 (1968).
[35]D. P. Hale, "Energy analysis of electron beams from perforated-mesh hollow-cathode gas discharge guns," Journal of Physics D: Applied Physics **4**, 1281 (1971).
[36]C. T. Teodorescu-Soare, D. G. Dimitriu, C. Ionita, and R. W. Schrittwieser, "Experimental investigations of the nonlinear dynamics of a complex space-charge configuration inside and around a grid cathode with hole," Physica Scripta **91**, 034002 (2016).
[37]R. W. Schrittwieser, C. Ionita, C. T. Teodorescu-Soare, O. Vasilovici, S. Gurlui, S. A. Irimiciuc, and D. G. Dimitriu, "Spectral and electrical diagnosis of complex space-charge structures excited by a spherical grid cathode with orifice," Physica Scripta **92**, 044001 (2017).
[38]Y. Ralchenko, R. K. Janev, T. Kato, D. V. Fursa, I. Bray, and F. J. De Heer, "Electron-impact excitation and ionization cross sections for ground state and excited helium atoms," Atomic Data and Nuclear Data Tables **94**, 603–622 (2008).
[39]H. C. Hayden and N. G. Utterback, "Ionization of helium, neon, and nitrogen by helium atoms," Physical Review **135**, A1575 (1964).
[40]M. Ohnishi, C. Hoshino, K. Masuda, Y. Yamamoto, H. Toku, and K. Yoshikawa, "Electron streaming from central core region in inertial-electrostatic confinement fusion," in *18th Symposium on Fusion Engineering, 1999* (IEEE, 1999) pp. 213–216.
[41]A. Phelps, "Lxcat database," (2013).
[42]M. J. Brunger, S. J. Buckman, L. J. Allen, I. E. McCarthey, and K. Ratnavelu, "Elastic scattering from helium: absolute experimental cross sections, theory and derived interaction potentials," Journal of Physics B: Atomic, Molecular and Optical Physics **25**, 1823 (1992).
[43]R. H. J. Jansen, F. J. De Heer, H. J. Luyken, B. Van Wingerden, and H. J. Blaauw, "Absolute differential cross sections for elastic scattering of electrons by helium, neon, argon and molecular nitrogen," Journal of Physics B: Atomic, Molecular and Optical Physics **9**, 185 (1976).
[44]S. Humphries, *Charged particle beams* (Courier Corporation, 2013) p. 318.
[45]I. Langmuir, "The interaction of electron and positive ion space charges in cathode sheaths," Physical Review **33**, 954 (1929).
[46]S. D. Baalrud, N. Hershkowitz, and B. Longmier, "Global nonambipolar flow: Plasma confinement where all electrons are lost to one boundary and all positive ions to another boundary," Physics of plasmas **14**, 042109 (2007).
[47]E. Oks, *Plasma cathode electron sources: physics, technology, applications* (John Wiley & Sons, 2006).
[48]S. P. Nikulin, "The effect of the anode dimensions on the characteristics of a hollow-cathode glow discharge," Technical Physics **42**, 495–498 (1997).
[49]W. Krug, "Eine neue glimmentladungserscheinung und ihre anwendungsmöglichkeit für braunsche röhren mit niedrigen kathodenspannungen," Archiv für Elektrotechnik **30**, 157–183 (1936).
[50]D. Levko, "Unmagnetized fireballs in the hollow cathode geometry," Physics of Plasmas **24**, 053514 (2017).
[51]J. Rocca, J. Meyer, and G. Collins, "Hollow cathode electron gun for the excitation of cw lasers," Physics Letters A **87**, 237–239 (1982).

[52] J. J. Rocca, J. D. Meyer, M. R. Farrell, and G. J. Collins, "Glow-discharge-created electron beams: Cathode materials, electron gun designs, and technological applications," Journal of applied physics **56**, 790–797 (1984).
[53] M. Yousefi, V. Damideh, and H. Ghomi, "Low-energy electron beam extraction from spherical discharge," IEEE Transactions on Plasma Science **39**, 2554–2555 (2011).
[54] B. Ulmen, *Formation and extraction of a dense plasma jet from a helicon-plasma-injected inertial electrostatic confinement device (Doctoral dissertation)*, Ph.D. thesis, University of Illinois at Urbana-Champaign (2014).

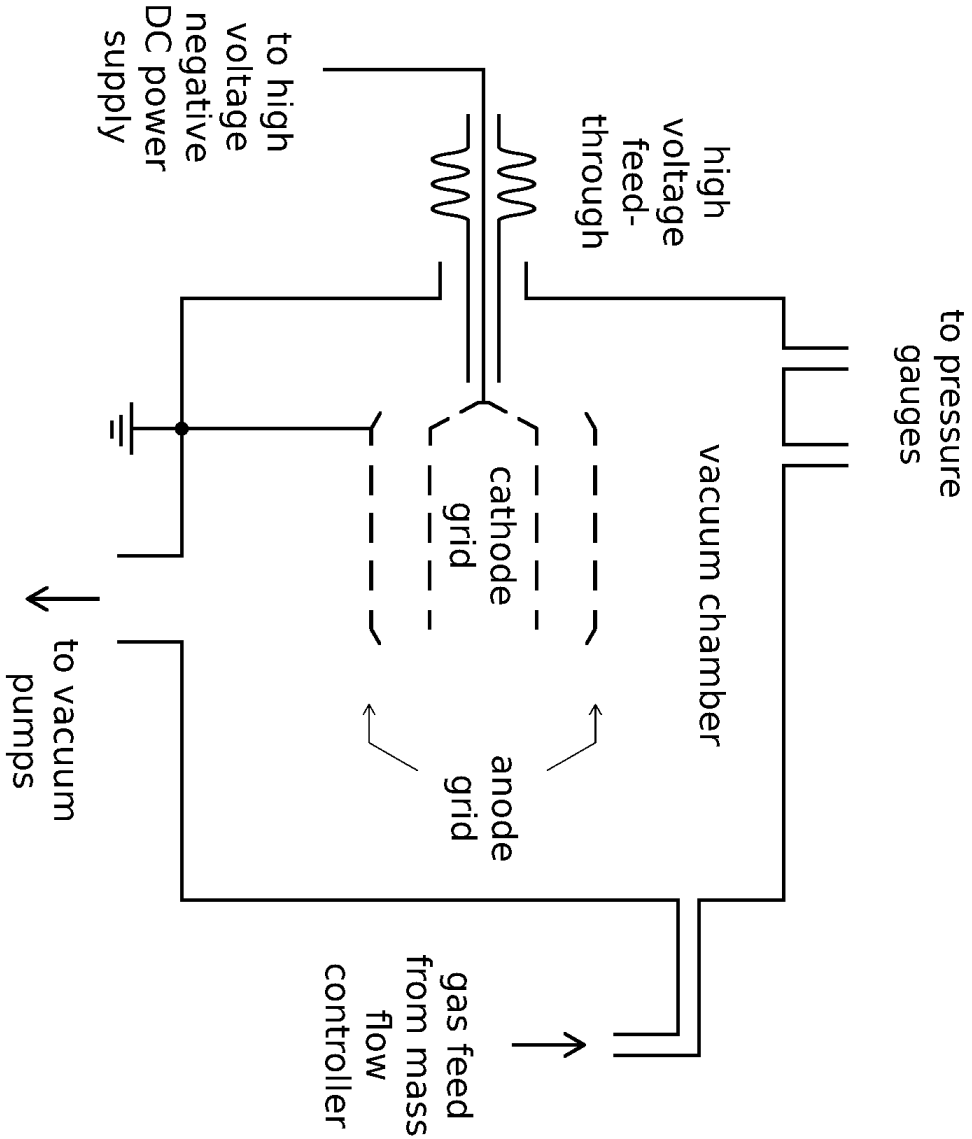

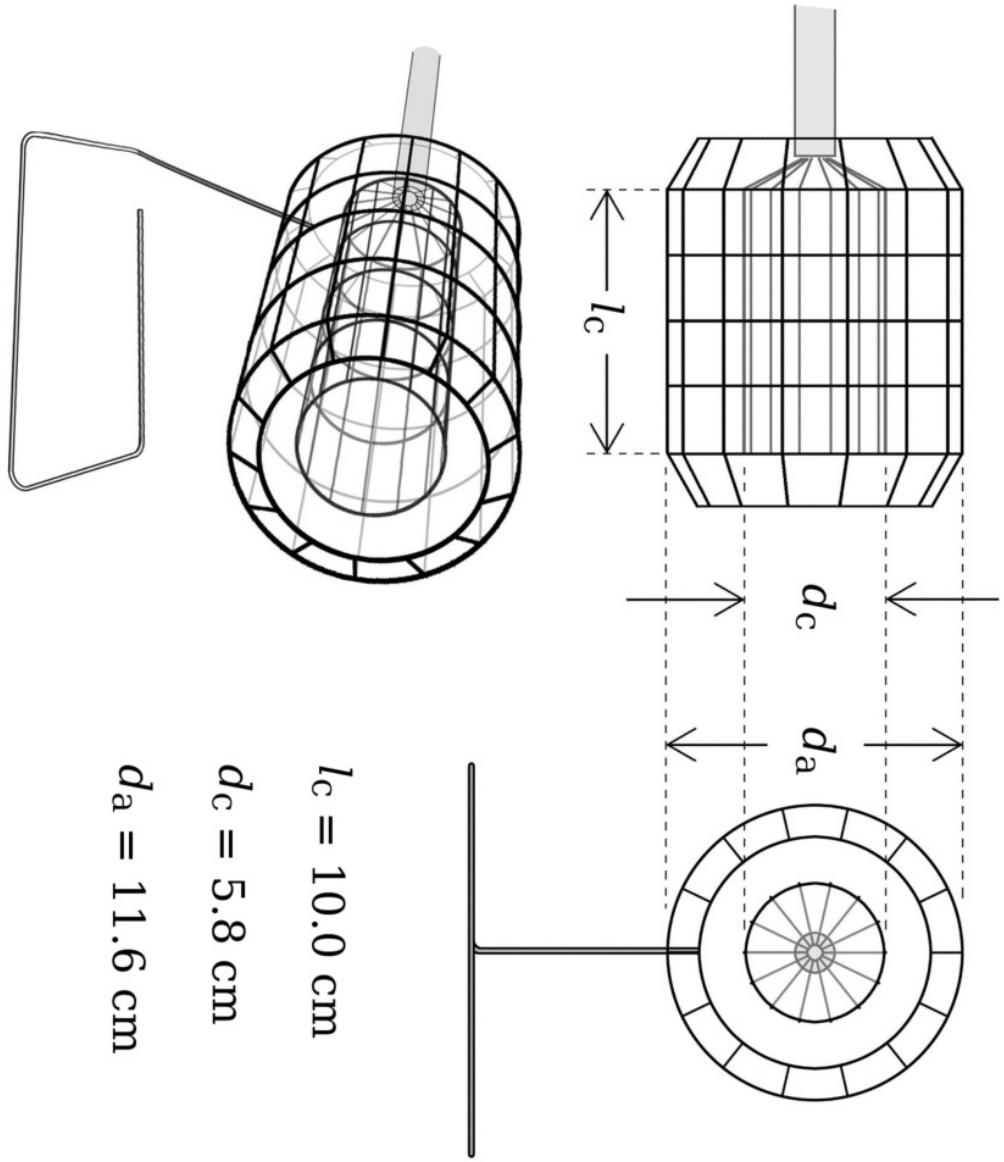

PLEASE CITE THIS ARTICLE AS DOI: 10.1063/1.5143310

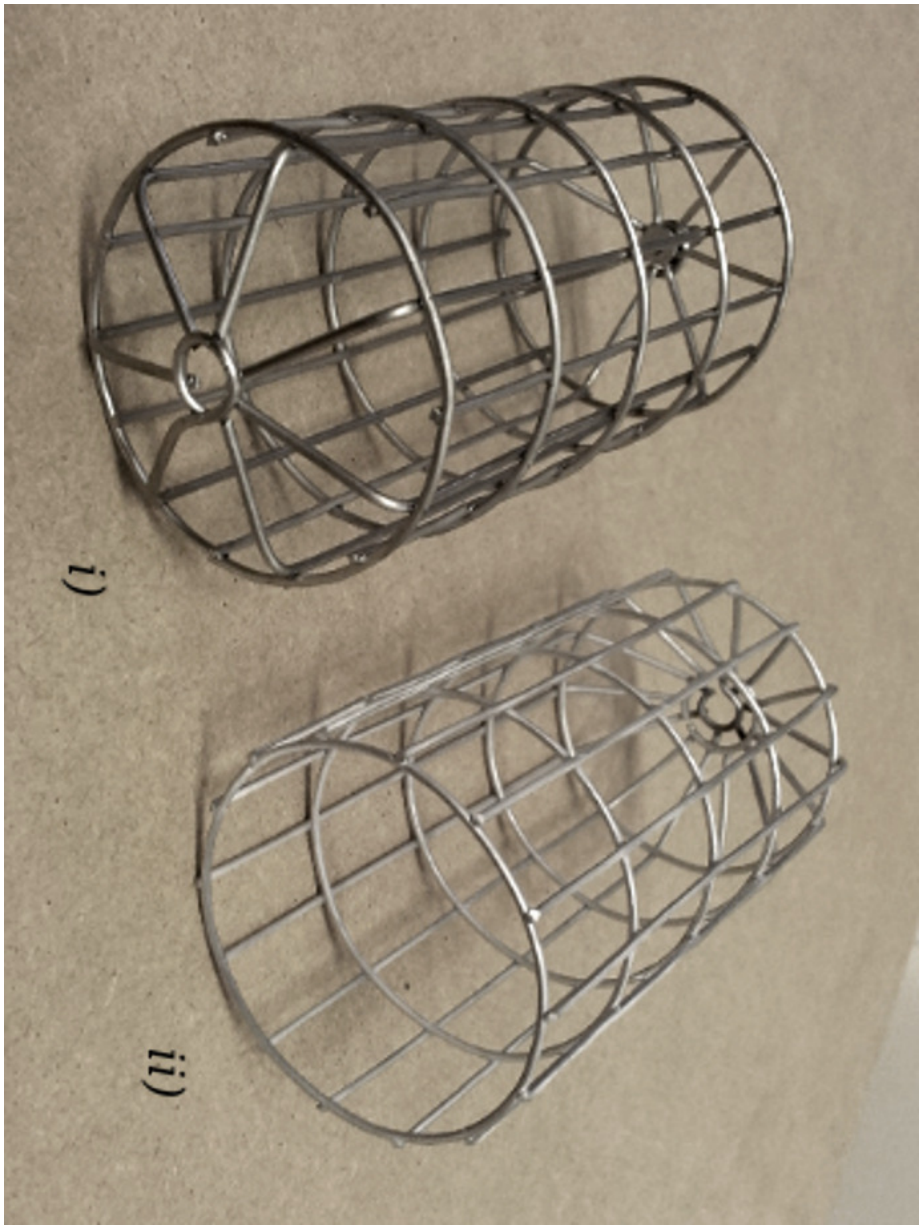

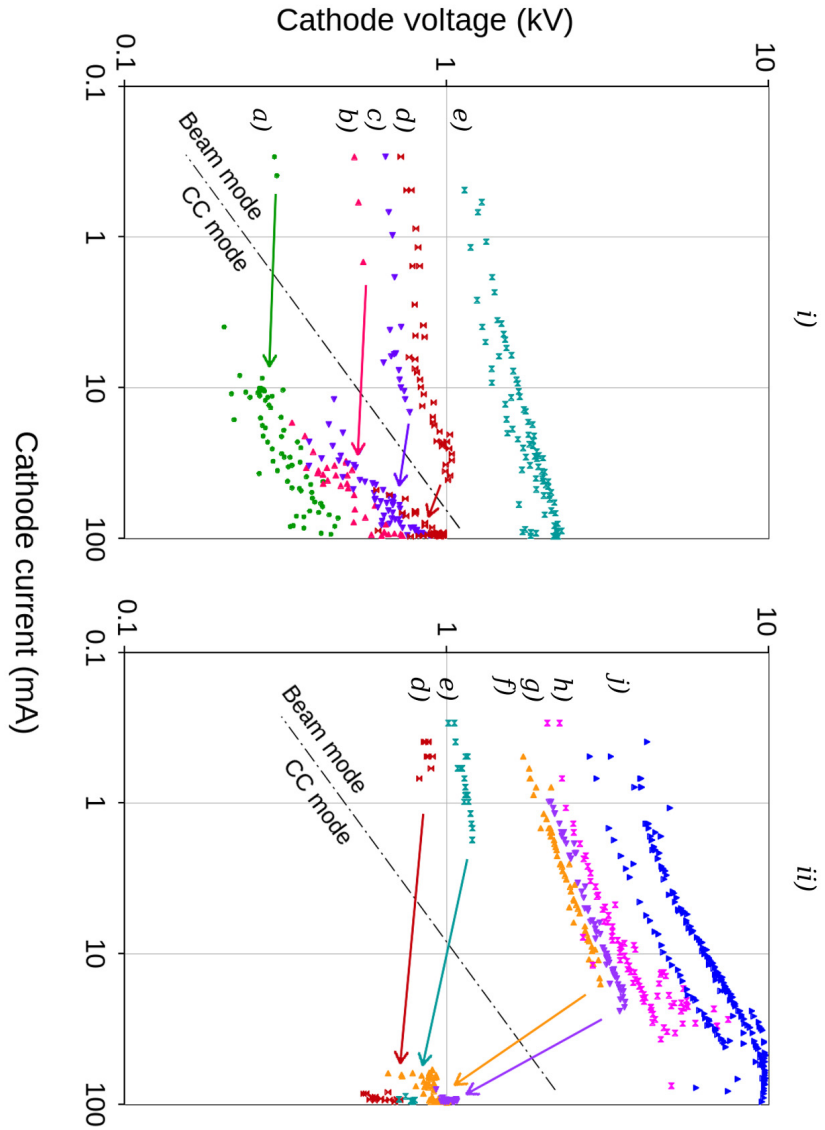

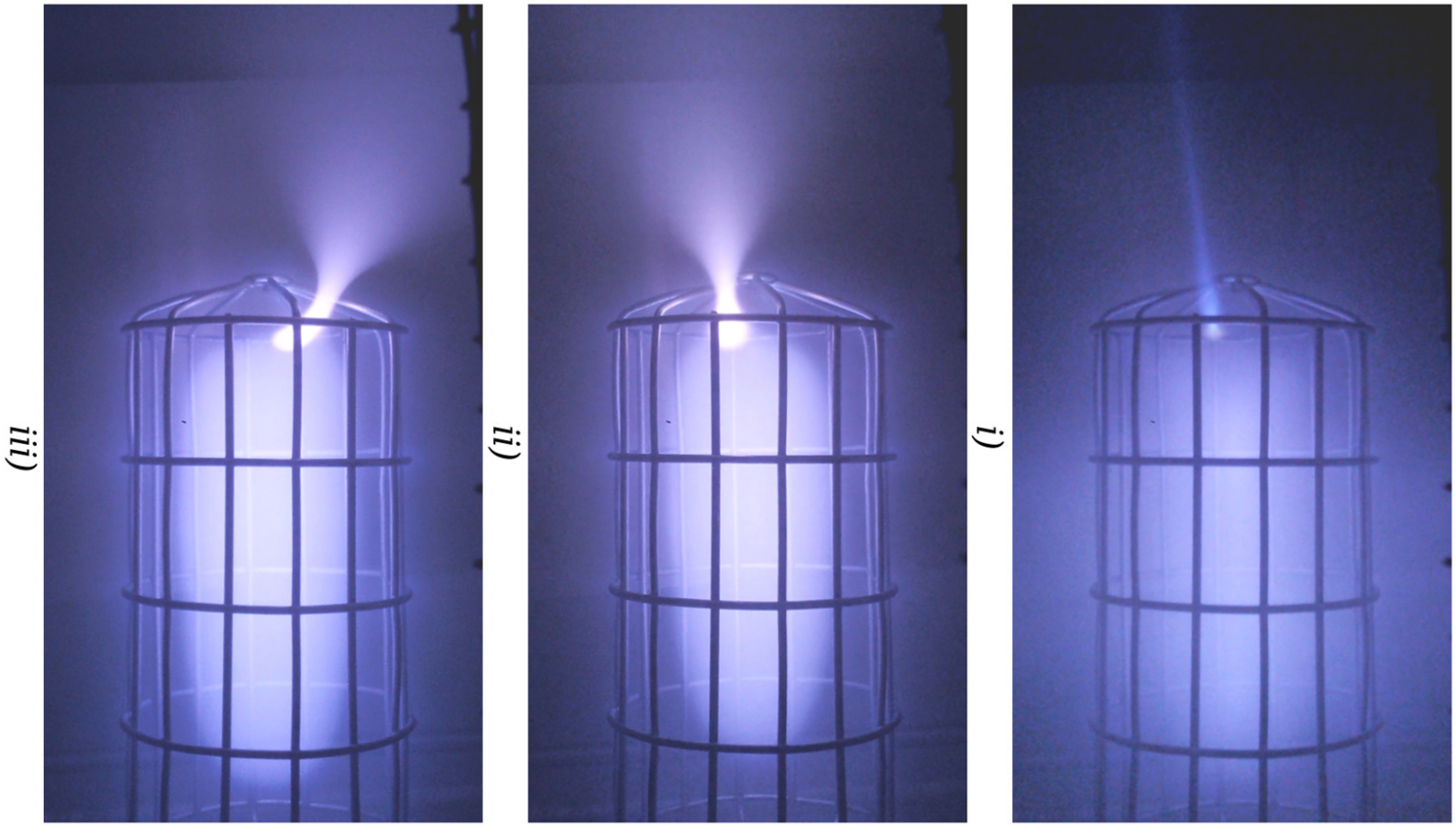

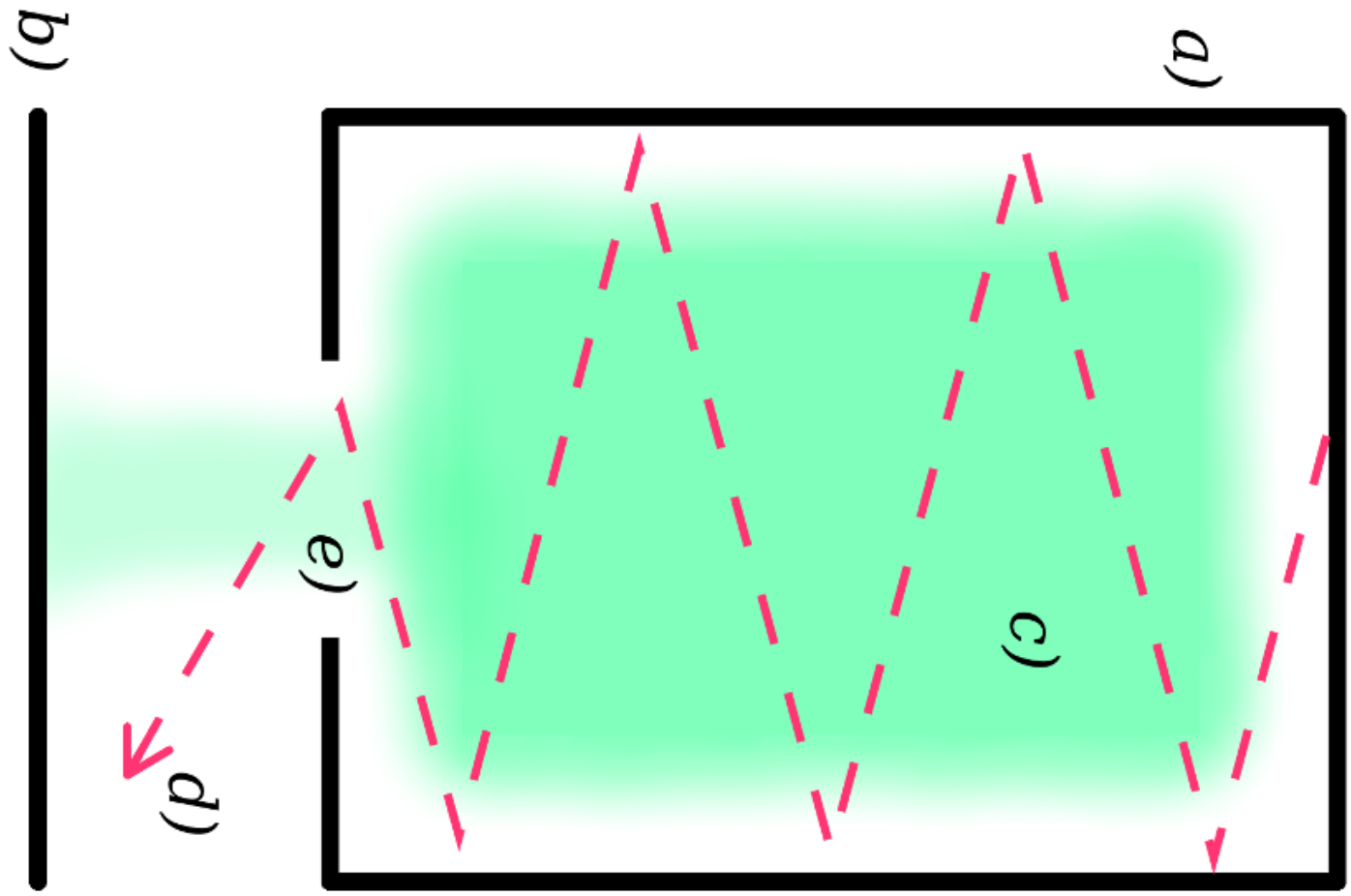

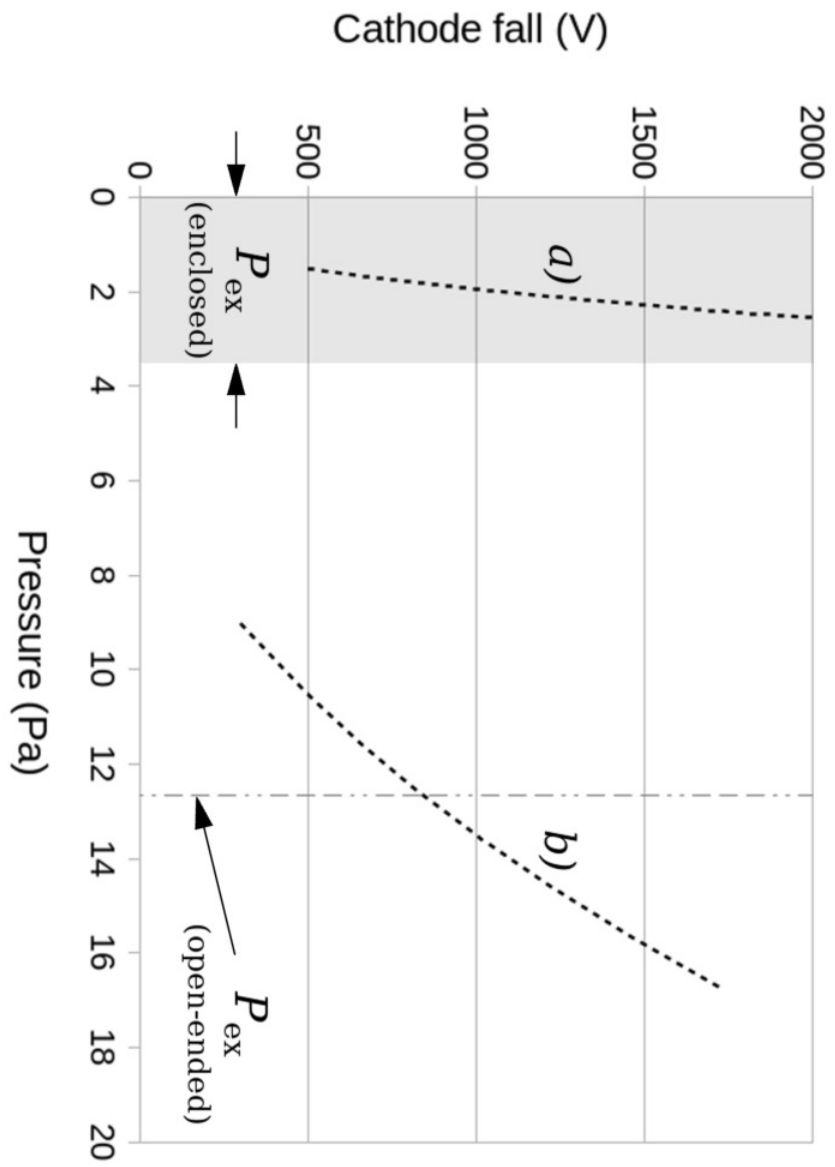

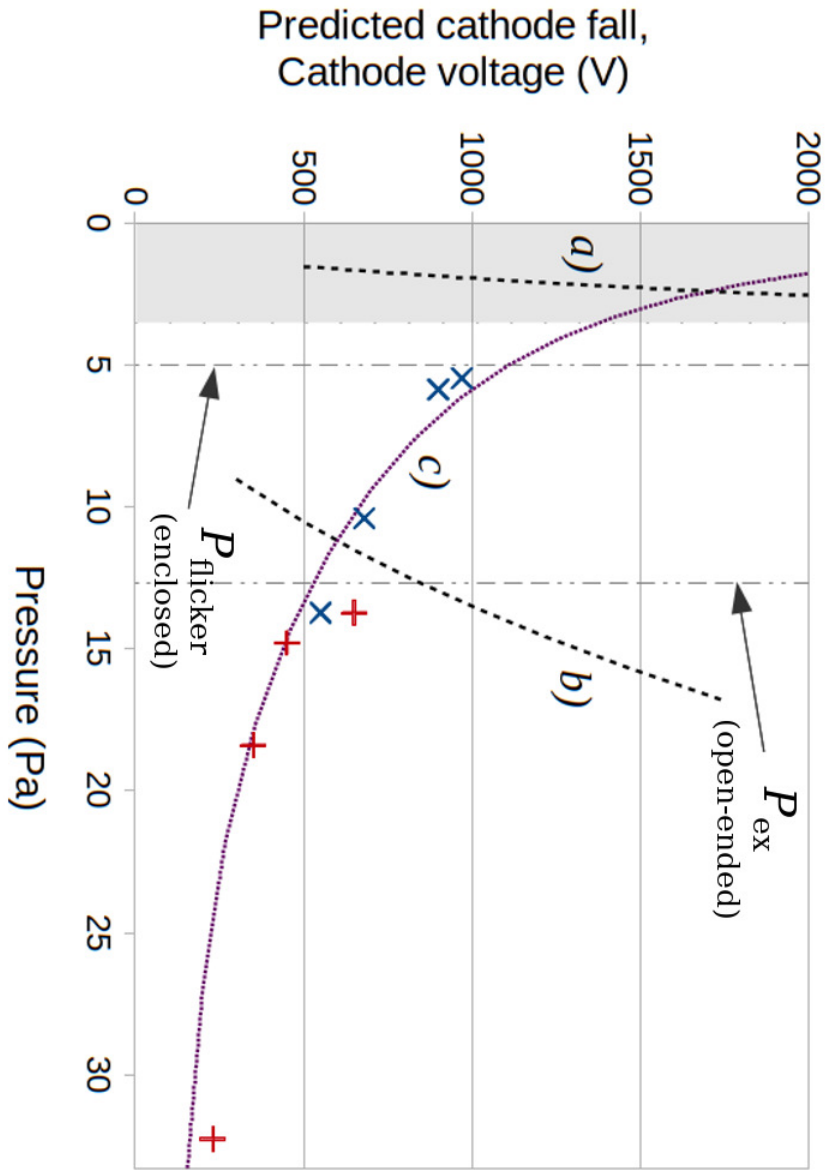

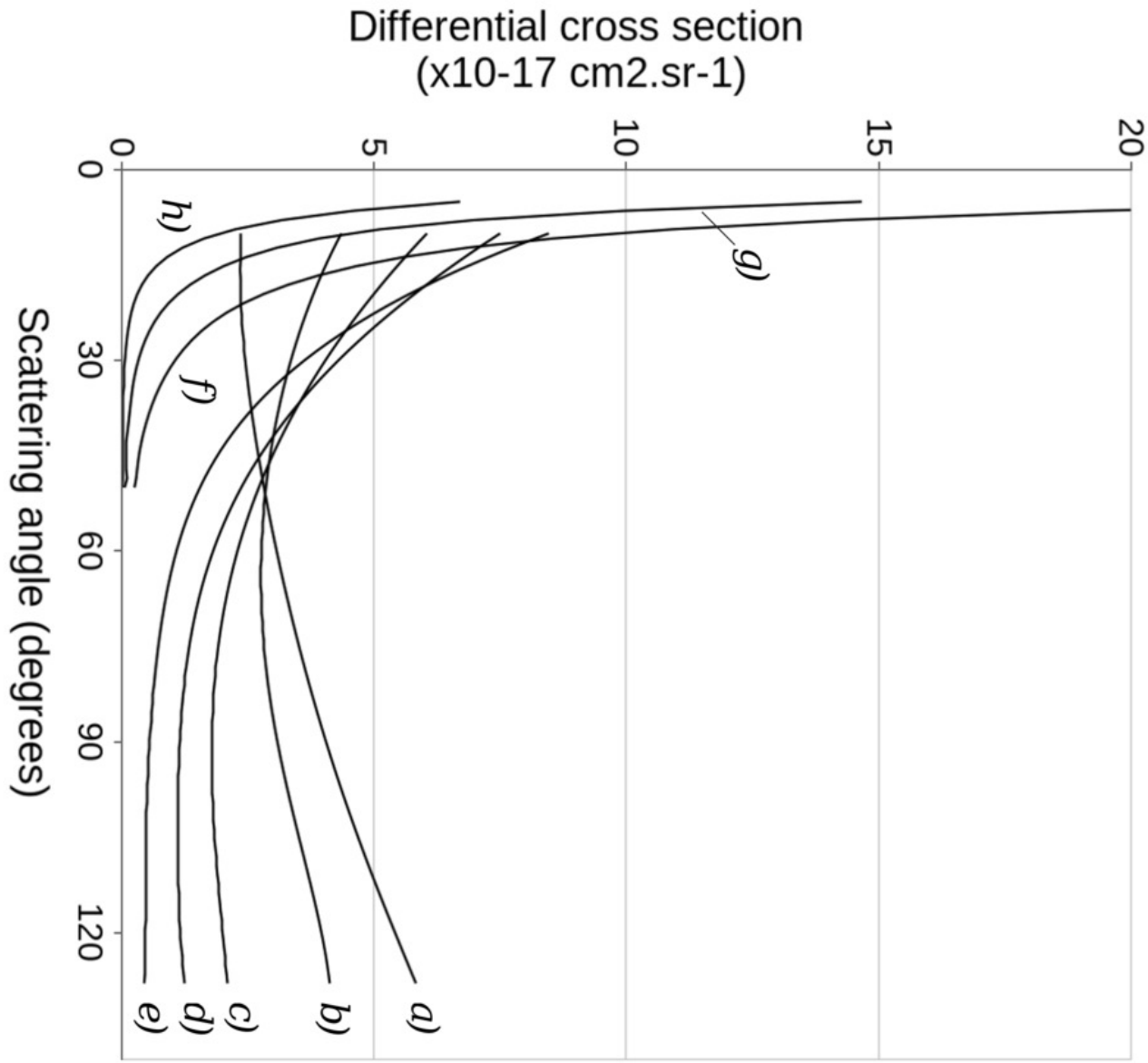

PLEASE CITE THIS ARTICLE AS DOI: 10.1063/1.5143310